

Superconvergence of gradient recovery on deviated discretized manifolds*

GUOZHI DONG^{1,2} AND HAILONG GUO³

¹Institute for Mathematics, Humboldt University of Berlin, Unter den Linden 6,
10099 Berlin, Germany

²Weierstrass Institute for Applied Analysis and Stochastics, Mohrenstrass 39,
10117 Berlin, Germany

³School of Mathematics and Statistics, The University of Melbourne, Parkville,
VIC, 3010, Australia

Abstract

This paper addresses open questions proposed by Wei, Chen and Huang [SIAM J. Numer. Anal., 48(2010), pp. 1920–1943]. Mainly two questions arise there: (i) How to design gradient recovery algorithms given no exact information of the underline surfaces; (ii) Whether the superconvergence still holds when the vertices of the triangle mesh have $\mathcal{O}(h^2)$ deviation to the underline exact surfaces. We positively answer both questions. For the first, we propose a family of isoparametric gradient recovery schemes, which turn out to be nature generalizations of classical recovery methods from the Euclidean domain to manifolds. For the second, we prove a property called geometric supercloseness condition, which subsequently leads to the desired superconvergence result. Numerical results are documented for verification.

AMS subject classifications. 41A25, 65N15, 65N30

Key words. Gradient recovery, manifolds, geometric supercloseness, superconvergence, isoparametric gradient recovery method, PPPR method, ZZ-scheme.

1 Introduction

Gradient recovery schemes for data defined in Euclidean domain have been intensively investigated [3, 22, 1, 14, 16, 23, 24, 25], and also find many interesting applications, e.g. [13, 19, 18, 15, 5]. The methods for data on discretized manifolds has been recently studied, e.g., in [12, 21, 13]. By looking into the literature, many of the recovery algorithms in the setting of Euclidean domain can be generalized to manifolds setting. However, it has some restriction that the exact geometry-prior (exact vertices, exact normal vectors) are needed either in the designing of the algorithms or in proving the superconvergence.

In the paper [21], Wei, Chen and Huang asked the following two questions: (i) How to design gradient recovery algorithms given no exact information of the surfaces (i.e., no exact normal fields, and no exact vertices); (ii) If such a recovery can be designed, then does it have superconvergence with triangulated meshes whose vertices located in a $\mathcal{O}(h^2)$ neighborhoods of the underline exact surfaces, where h is the scale of the mesh size. In [10], the authors proposed a recovery scheme called parametric polynomial preserving recovery method, which does not rely on the exact geometry-prior, and it was proven to be able to achieve superconvergence under mildly structured meshes, including high curvature cases. That can be thought of as an answer to the first question. Still, the theoretical proof for the superconvergence there requires the vertices to be located on the exact manifolds, though numerically the superconvergence has been observed even the vertices not sitting on the exact manifolds.

*Emails: guozhi.dong@hu-berlin.de/guozhi.dong@wias-berlin.de; hailong.guo@unimelb.edu.au

This paper aims to solve this problem. To do this, we introduce the concept of geometric supercloseness, which can be theoretically justified under the $\mathcal{O}(h^2)$ vertex condition. Another contribution is that we generalize the idea in [10] of using a parametric domain for polynomial preserving recovery on manifolds to other standard recovery schemes [21]. In this vein, we develop a family of parametric recovery schemes for data on discretized manifolds. It consists of two-level recoveries: one is recovering the Jacobian of local geometric mapping over the parametric domain, and the other is recovering the data gradient iso-parametrically to the geometric parametrization.

The paper is organized as follows: In Section 2, we describe the general geometric setting of this paper, where we prove the geometric supercloseness result. In Section 3, we provide the framework for the family of isoparametric gradient recovery schemes. In Section 4, we prove the superconvergence of the recovery scheme. Finally, we show numerical examples which verifies the theoretical result in Section 5.

2 Geometric supercloseness

We first specify in the beginning of this section some of the geometrical objectives and notations involved in the paper, and then prove a property called geometric supercloseness from the approximation conditions.

2.1 Geometric setting

\mathcal{M} is a general d -dimensional C^3 smooth compact hypersurface embedded in \mathbb{R}^{d+1} , and $\mathcal{M}_h = \bigcup_{j \in J_h} \tau_{h,j}$ is a polytope approximation of \mathcal{M} , with $h = \max_{j \in J_h} \text{diam}(\tau_{h,j})$ the maximum diameter of the triangles $\tau_{h,j}$. Here J_h and I_h are the index sets for triangles and vertices of \mathcal{M}_h , respectively. We denote $\{\tau_j\}_{j \in J_h}$ the corresponding curved triangles which satisfy $\bigcup_{j \in J_h} \tau_j = \mathcal{M}$. Note that the vertices of \mathcal{M}_h do not necessarily locate on \mathcal{M} , therefore τ_j and $\tau_{h,j}$ may have no common vertices. In the following study, we introduce \mathcal{M}_h^* to be the counterpart of \mathcal{M}_h with the same number of vertices, all of which are located on \mathcal{M} . To obtain \mathcal{M}_h^* , we project $\{x_{h,i}\}_{i \in I_h}$ the vertices of \mathcal{M}_h along unit normal direction of \mathcal{M} to have $\{x_{h,i}^*\}_{i \in I_h}$ the vertices of \mathcal{M}_h^* . Then we connect $\{x_{h,i}^*\}_{i \in I_h}$ using the same order as the connection of $\{x_{h,i}\}_{i \in I_h}$, which gives the triangulation of \mathcal{M}_h^* . $\{\tau_{h,j}^*\}_{j \in J_h}$ denote the corresponding triangles on \mathcal{M}_h^* . We focus on linear finite element methods in order to better illustrating the idea, thus the nodes consist of simply all the vertices of \mathcal{M}_h .

In [21], gradient recovery methods are generalized from planar domain to surfaces, while it is restricted to the case that the vertices are located on the underline exact surface. That is, it has been only studied the case that the discretization are given by, corresponding to our notation, \mathcal{M}_h^* . It has been, however, conjectured that the superconvergence of gradient recovery on general discretized surfaces, like \mathcal{M}_h , may be proven if the vertices of \mathcal{M}_h are in a $\mathcal{O}(h^2)$ neighborhood of the corresponding vertices of \mathcal{M}_h^* . That is the following vertex-deviation condition

$$|x_{h,i}^* - x_{h,i}| = \mathcal{O}(h^2) \quad \text{for all } i \in I_h. \quad (2.1)$$

We recall the transform operators between the function spaces on \mathcal{M} and on \mathcal{M}_h (or similarly \mathcal{M}_h^*). Let $\mathcal{V}(\mathcal{M})$ and $\mathcal{V}(\mathcal{M}_h)$ be some ansatz function spaces, then we define the transform operators

$$\begin{aligned} T_h : \mathcal{V}(\mathcal{M}) &\rightarrow \mathcal{V}(\mathcal{M}_h); & (T_h)^{-1} : \mathcal{V}(\mathcal{M}_h) &\rightarrow \mathcal{V}(\mathcal{M}); \\ v &\mapsto v \circ \Gamma_h, & \text{and} & & v_h &\mapsto v_h \circ \Gamma_h^{-1}, \end{aligned} \quad (2.2)$$

where Γ_h is an affine map from every element in $\{\tau_{h,j}\}_{j \in J_h}$ to the corresponding element in $\{\tau_j\}_{j \in J_h}$. The operators $(T_h^*)^\pm$ between functions on \mathcal{M} and \mathcal{M}_h^* are similarly defined.

In the following analysis, at each vertex $x_{h,i}^*$, a local parametrization function $\mathbf{r}_i : \Omega_i \rightarrow \mathcal{M}$ is needed, which maps an open set in the parameter domain $\Omega_i \subset \mathbb{R}^d$ to an open set around $x_{h,i}^*$ on the manifold. Note that we take Ω_i a compact set which is the parameter domain corresponding to the selected patch on \mathcal{M}_h^* around the vertex $x_{h,i}^*$, or respectively the patch on \mathcal{M}_h around the vertex $x_{h,i}$.

In such a way, we define local parametrization functions $\mathbf{r}_{h,i} : \Omega_i \rightarrow \mathcal{M}_h$ and $\mathbf{r}_{h,i}^* : \Omega_i \rightarrow \mathcal{M}_h^*$, respectively. They are piece-wise linear functions. In addition, we use $\mathbf{r}_{\tau_{h,j}} : \tau_{h,j} \rightarrow \tau_j$ and $\mathbf{r}_{\tau_{h,j}}^* : \tau_{h,j}^* \rightarrow \tau_j$ to denote the local parameterizations from the small triangle pairs $\tau_{h,j}$ and τ_j to τ_j , respectively. Due to the smoothness assumption on \mathcal{M} , \mathbf{r}_i , $\mathbf{r}_{\tau_{h,j}}$ and $\mathbf{r}_{\tau_{h,j}}^*$ all are C^3 functions for every $i \in I_h$ and $j \in J_h$. Particularly, it implies that $\mathbf{r}_i \in W^{3,\infty}(\Omega_i)$ and $\mathbf{r}_{\tau_{h,j}} \in W^{3,\infty}(\tau_{h,j})$ and $\mathbf{r}_{\tau_{h,j}}^* \in W^{3,\infty}(\tau_{h,j}^*)$, respectively. The condition (2.1) indicates that triangulated surface \mathcal{M}_h converges to \mathcal{M} as $h \rightarrow 0$.

2.2 Supercloseness of geometric approximation

In this part, we prove some approximation properties on the paired triangular meshes \mathcal{M}_h and \mathcal{M}_h^* . We introduce some relevant definitions first.

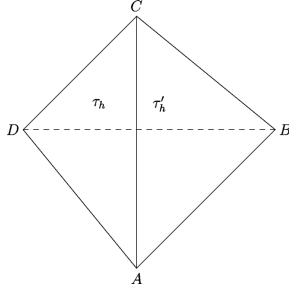


Figure 1: Illustration of two adjacent triangles.

Definition 2.1. Suppose τ_h and τ'_h are two adjacent triangles in \mathcal{T}_h , as illustrated in Figure 1. They are said to form an $\mathcal{O}(h^2)$ parallelogram if

$$|\overrightarrow{AB} - \overrightarrow{CD}| = \mathcal{O}(h^2), \quad \text{and} \quad |\overrightarrow{BC} - \overrightarrow{DA}| = \mathcal{O}(h^2).$$

Definition 2.2. A triangular mesh \mathcal{T}_h is said to satisfy the $\mathcal{O}(h^{2\sigma})$ irregular condition if there exist a partition $\mathcal{T}_{h,1} \cup \mathcal{T}_{h,2}$ of \mathcal{T}_h and a positive constant σ such that every two adjacent triangles in $\mathcal{T}_{h,1}$ form an $\mathcal{O}(h^2)$ parallelogram and

$$\sum_{\tau_h \in \mathcal{T}_{h,2}} |\tau_h| = \mathcal{O}(h^{2\sigma}).$$

Before going further, we make some standard assumptions on the meshes.

Assumption 2.3. (i) The triangulation \mathcal{M}_h is shape regular and quasi-uniform. Moreover, the $\mathcal{O}(h^{2\sigma})$ irregular condition holds for \mathcal{M}_h .

(ii) \mathcal{M}_h and \mathcal{M}_h^* have the same amount of triangles and vertices, and every vertex pair of \mathcal{M}_h and \mathcal{M}_h^* satisfy the deviation bound in (2.1).

The first condition of Assumption 2.3 is quite standard, and it is crucial for proving superconvergence in the literature, e.g., [3, 22, 21]. However, in the manifold setting, this condition has been assumed on \mathcal{M}_h^* , that is the exact interpolation of \mathcal{M} . In the following, we show that with Assumption 2.3, it implies a geometric approximation property which we call it **geometric supercloseness**. We need some auxiliary results which are given in the following lemma.

Lemma 2.4. Let τ_1 and τ_2 both be shape regular triangles of diameter h , and the distance between their vertex-pairs is of order h^2 , where $h \ll 1$. Let $\Gamma : \tau_1 \rightarrow \tau_2$ be the affine transformation, and its Jacobian $\partial\Gamma$ consists of orthogonal vectors $\{\partial_k \Gamma\}_{k=1,\dots,d}$. Then we have following relations:

$$\|\partial\Gamma - \text{Id}\|_{\infty, \tau_1} = \mathcal{O}(h^2). \quad (2.3)$$

and

$$|\sqrt{\det((\partial\Gamma)^\top \partial\Gamma)} - 1| = \mathcal{O}(h^2). \quad (2.4)$$

Proof. Since $(\partial\Gamma + \text{Id})^\top$ is a bounded linear map and has a bounded generalized inverse, we have

$$|\partial\Gamma - \text{Id}| \sim |(\partial\Gamma)^\top \partial\Gamma - \text{I}|.$$

Here I is the $d \times d$ identity matrix. Due to the orthogonality, we have

$$(\partial\Gamma)^\top \partial\Gamma = [\partial_k \Gamma \cdot \partial_k \Gamma]$$

where $[\partial_k \Gamma \cdot \partial_k \Gamma]$ denotes the diagonal matrix with the element $\partial_k \Gamma \cdot \partial_k \Gamma$ on its diagonals.

Because of our assumption on the vertices of τ_1 and τ_2 , we have that

$$\partial_k \Gamma \cdot \partial_k \Gamma \leq \frac{h^2 + c_k h^4}{h^2} \leq 1 + c_k h^2, \quad \text{for all } k = 1, \dots, d$$

for some constant c_k either positive or negative. By definition of matrix norm, we have $\|[\partial_k \Gamma \cdot \partial_k \Gamma] - \text{I}\| = \max_k \{\partial_k \Gamma \cdot \partial_k \Gamma - 1\}$. Thus we have

$$|\partial\Gamma - \text{Id}| \leq C \max_k \{\partial_k \Gamma \cdot \partial_k \Gamma - 1\} \leq C|c|h^2$$

and this give the relation in (2.3). For (2.4), notice $\mathcal{A}(\tau_2) = \sqrt{\det([\partial_k \Gamma \cdot \partial_k \Gamma])} \mathcal{A}(\tau_1)$. Then $\sqrt{\det([\partial_k \Gamma \cdot \partial_k \Gamma])} = \frac{\mathcal{A}(\tau_2)}{\mathcal{A}(\tau_1)}$. Due to the area difference of the two triangles τ_1 and τ_2 , we have

$$\frac{\mathcal{A}(\tau_2)}{\mathcal{A}(\tau_1)} = \sqrt{\prod_k \partial_k \Gamma \cdot \partial_k \Gamma} \leq \sqrt{\prod_k (1 + c_k h^2)} \sim 1 + ch^2$$

for h sufficiently small. \square

Note that the orthogonality of $\partial_k \Gamma$ is not essential. This is because if we take other local bases for computing the Jacobian, then the new tensor matrix will be equivalent to the diagonal matrix. Precisely we have $|B| = |A|$ for $B = U^\top A U$, where A is a diagonal matrix, and B is a symmetric matrix, and U is some unitary matrix.

Proposition 2.5. *Let \mathcal{M}_h and \mathcal{M}_h^* satisfy Assumption 2.3, then we have*

- (i) *The triangulation \mathcal{M}_h^* is also shape regular and quasi-uniform, and the $\mathcal{O}(h^{2\sigma})$ irregular condition is fulfilled for \mathcal{M}_h^* .*
- (ii) *The local piece-wise linear parametrization functions, $\mathbf{r}_{h,i}$ and $\mathbf{r}_{h,i}^*$, satisfy*

$$\|\partial \mathbf{r}_{h,i} - \partial \mathbf{r}_{h,i}^*\|_{0,\Omega_i} = \sqrt{\mathcal{A}(\mathcal{M}_{h,i}^*)} \mathcal{O}(h^2), \quad \text{for all } i \in I_h. \quad (2.5)$$

Here \mathcal{A} is the area functional, and $\mathcal{M}_{h,i}^* \subset \mathcal{M}_h^*$ is the patch corresponding to the parameter domain Ω_i .

Proof. The first assertion is not hard to verify by considering the definition of shape regular and quasi-uniform, which can be found in many textbooks of finite element methods [4, 6], and also the definition of the $\mathcal{O}(h^{2\sigma})$ irregular condition above.

Now we prove the second assertion. Let Ω_i be the parameter domain for patches selected around the vertex $x_{h,i}$. Denote the local index-set associated to vertices of the selected patch around $x_{h,i}$ to be J_i . We notice that both $\mathbf{r}_{h,i}$ and $\mathbf{r}_{h,i}^*$ are piecewise linear functions defined on Ω_i . Let $\Omega_{i,j}$ be the common parameter domain for the corresponding triangle pairs $\tau_{h,j}$ and $\tau_{h,j}^*$ for the index $j \in J_i$. Then $\mathbf{r}_{h,i}$ and $\mathbf{r}_{h,i}^*$ are linear functions on each of the regions $\Omega_{i,j}$ for every $j \in J_i$.

Thus the Jacobian $\partial \mathbf{r}_{h,i}$ and $\partial \mathbf{r}_{h,i}^*$ will be constant functions, and we have

$$\|\partial \mathbf{r}_{h,i} - \partial \mathbf{r}_{h,i}^*\|_{0,\Omega_{i,j}} \leq |\partial \mathbf{r}_{h,i}^*| \|\partial \mathbf{r}_{h,i} (\partial \mathbf{r}_{h,i}^*)^\dagger - \text{Id}\|_{0,\tau_{h,j}^*} \leq C \|\partial \mathbf{r}_{h,i} (\partial \mathbf{r}_{h,i}^*)^\dagger - \text{Id}\|_{0,\tau_{h,j}^*}.$$

Due to the geometric regularity assumption that \mathcal{M} has bounded curvature, thus all the elements $\{|\partial \mathbf{r}_{h,i}^*|\}_{i \in I_h}$ are uniformly bounded from below and from above given $\{\Omega_i\}_{i \in I_h}$. On the other hand, $\partial \mathbf{r}_{h,i} (\partial \mathbf{r}_{h,i}^*)^\dagger$ is also a constant function. It is the Jacobian of the linear geometric function

which maps $\tau_{h,j}^*$ to $\tau_{h,j}$. We denote this map by Γ_j . Then we have $\partial\Gamma_j = \partial\mathbf{r}_{h,i}(\partial\mathbf{r}_{h,i}^*)^\dagger$. Therefore we have

$$\|\partial\mathbf{r}_{h,i}(\partial\mathbf{r}_{h,i}^*)^\dagger - \text{Id}\|_{0,\tau_{h,j}^*} = \|\partial\Gamma_j - \text{Id}\|_{0,\tau_{h,j}^*}.$$

Apply the result from Lemma 2.4, we have

$$\|\partial\mathbf{r}_{h,i} - \partial\mathbf{r}_{h,i}^*\|_{0,\Omega_{i,j}} \leq C\sqrt{\mathcal{A}(\tau_{h,j}^*)}h^2.$$

Summing up over $j \in J_i$ we arrive the following inequality

$$\|\partial\mathbf{r}_{h,i} - \partial\mathbf{r}_{h,i}^*\|_{0,\Omega_i}^2 = \sum_{j \in J_i} \|\partial\mathbf{r}_{h,i} - \partial\mathbf{r}_{h,i}^*\|_{0,\Omega_{i,j}}^2 = \mathcal{O}(h^4) \sum_{j \in J_i} \mathcal{A}(\tau_{h,j}^*).$$

Taking square root on both sides gives the conclusion of the second assertion. \square

The relation in (2.5) tells in fact some regularity on the approximations of \mathcal{M}_h to \mathcal{M} . It is similar to the supercloseness property for the the gradient of the finite element solutions to the interpolation of the exact solutions.

3 Isoparametric gradient recovery schemes on manifolds

Here, we generalize the idea of parametric polynomial preserving recovery proposed in [10] to have a general family of recovery methods in manifolds setting. More precisely, the algorithm framework we provide here generalize of the methods introduced in [21], which ask for exact geometry-prior, to the case without exact geometry-prior. To do this, we rely on the intrinsic definition of gradient operator on manifolds. Given a local parametric patch, and $\mathbf{r} : \Omega \rightarrow \mathcal{M}$ the parametrization function of this patch, define $\bar{u} := u \circ \mathbf{r}$, then we have

$$(\nabla_g u) \circ \mathbf{r} = \nabla \bar{u}(g \circ \mathbf{r})^{-1} \partial \mathbf{r} = \nabla \bar{u}(\partial \mathbf{r})^\dagger \quad \text{on } \Omega. \quad (3.1)$$

Here $(\partial \mathbf{r})^\dagger$ is the pseudo-inverse of the Jacobian $\partial \mathbf{r}$. For a small digest of differential operator on manifolds, we refer to the appendix of [11] and also the background part in [10]. One may refer to the textbooks, e.g., [9] for more comprehensive introduction on differential geometry. From (3.1), we have the idea that to recover the gradient on manifolds using a two-level strategy. That is to recover the Jacobian $\partial \mathbf{r}$ and also $\nabla \bar{u}$ iso-parametrically on every local patch. We call the new methods Isoparametric gradient recovery schemes. They ask for neither the exact vertices nor the precise tangent spaces. In particular the PPPR method introduced in [10] can also be put under the same umbrella.

Precisely, we have the following framework described in Algorithm 1 for a family of recovery methods. For simplicity, we focus on 2-dimensional cases.

Note that the nodes for the recovered gradients are not necessarily the vertices of the triangles, e.g., if one use the ZZ scheme for the local recovery at Step (3), and Step (4). On the other hand, since there has no concrete recovery schemes been specified in Step (3), and Step (4), almost all the local recovery methods for functions in Euclidean domain can be used. Though the preferred candidates will be ZZ-scheme and PPR. The latter gives then the PPPR method proposed in [10]. In view of (3.2), one can see that it is an approximation of (3.1) at every nodes: $R_h^k \bar{u}_{h,i}$ recovers $\nabla \bar{u}$, and $(J_{r,i})^\dagger(\phi_i^1, \phi_i^2, \phi_i^3)$, recovers $(\partial \mathbf{r})^\dagger$. We can also have the intuition that the result in (2.5) is required in order to match the superconvergence of the function gradient recovery and the superconvergence of the geometry Jacobian recovery, simultaneously.

In the next section, we will show the superconvergence property of the recovery scheme.

4 Superconvergence analysis with no exact geometry-prior

Even though we have shown a general algorithmic framework, which can cover several different methods under the same umbrella, for the theoretical analysis, we will focus on parametric polynomial preserving recovery scheme. It asks for less requirements on the meshes in comparison with several other methods, e.g., for simple (weighted) average, or generalized ZZ-scheme, an additional

Algorithm 1 Isoparametric gradient recovery schemes

Input: Discretized triangular surface \mathcal{M}_h and the data (FEM solutions) $(u_{h,i})_{i \in I_h}$. Then repeat steps (1) – (5) for all $i \in I_h$.

- (1) At every $x_{h,i}$, select a local patch $\mathcal{M}_{h,i} \in \mathcal{M}_h$ around $x_{h,i}$ with sufficient vertices. Compute the unit normal vectors of every triangle faces in $\mathcal{M}_{h,i}$. Compute the simple (weighted) average of the unit normal vectors, and normalize it to be ϕ_i^3 . Take the orthogonal space to ϕ_i^3 to be the parametric domain Ω_i . Shift $x_{h,i}$ to be the origin of Ω_i , and choose (ϕ_i^1, ϕ_i^2) the orthonormal basis of Ω_i .
- (2) Project all selected vertices of $\mathcal{M}_{h,i}$ onto the parametric domain Ω_i from Step (1), and record the new coordinates as $\zeta_{i,j}$.
- (3) Use a planar recovery scheme R_h^k to recover the surface Jacobian with respect to Ω_i . Typically, we consider every surface patch as local graph of some function s , that is $\mathbf{r}_i = (\Omega_i, s_i(\Omega_i))$. Then the recovered Jacobian at the selected patch is $J_{r,i} = (\mathbf{I}, R_h^k s_{i,j})^\top$, where \mathbf{I} is the identity matrix of the dimension Ω_i .
- (4) For every $\bar{u}_{h,i}$, using the same planar recovery scheme R_h^k to recover its gradient with respect to parameter domain Ω_i .
- (5) In the spirit of (3.1), use the results from Step (3) and Step (4) to get the recovered gradient at $x_{h,i}$:

$$G_h^k u_{h,i} = R_h^k \bar{u}_{h,i} (J_{r,i})^\dagger (\phi_i^1, \phi_i^2, \phi_i^3), \quad (3.2)$$

where $(J_{r,i})^\dagger = (J_{r,i} J_{r,i}^\top)^{-1} J_{r,i}$. The orthonormal basis $\{\phi_i^1, \phi_i^2, \phi_i^3\}$ is multiplied to unify the coordinates from local ones to a global one in the ambient Euclidean space.

Output: The recovered gradient at selected nodes $\{G_h^k u_{h,i}\}_{i \in I_h}$. For x being not a vertex of triangles, we use linear finite element basis to interpolate the values $\{G_h u_{h,i}\}_{i \in I_h}$ at vertices of each triangle.

$\mathcal{O}(h^2)$ -symmetric condition is required [10]. However, the general idea of the proof is extendable to the other methods as well.

We take the following Laplace-Beltrami equation as our model problem to implement the analysis.

$$-\Delta_g u = f \quad \text{where} \quad \int_{\mathcal{M}} f \, dvol = 0, \quad (4.1)$$

The weak formulation of equation (4.1) is given as follows: Find $u \in H^1(\mathcal{M})$ with $\int_{\mathcal{M}} u \, dvol = 0$ such that

$$\int_{\mathcal{M}} \nabla_g u \cdot \nabla_g v \, dvol = \int_{\mathcal{M}} f v \, dvol, \quad \text{for all } v \in H^1(\mathcal{M}). \quad (4.2)$$

The regularity of the solutions has been proved in [2, Chapter 4]. In the finite element methods, the surface \mathcal{M} is approximated by the triangulation \mathcal{M}_h which satisfy Assumption 2.3, and the solution is simulated in the piecewise linear function spaces \mathcal{V}_h defined over \mathcal{M}_h ,

$$\int_{\mathcal{M}_h} \nabla_{g_h} u_h \cdot \nabla_{g_h} v_h \, dvol_h = \int_{\mathcal{M}_h} f_h v_h \, dvol_h, \quad \text{for all } v_h \in \mathcal{V}_h(\mathcal{M}_h). \quad (4.3)$$

We first show that there exists an underline smooth manifold denoted by $\widetilde{\mathcal{M}}_h$ so that \mathcal{M}_h can be thought as an interpolation of it. This intermediate manifold is not needed practically in the algorithm, but it is helpful for our error analysis.

Proposition 4.1. *Let \mathcal{M} be the precise manifold, and \mathcal{M}_h and \mathcal{M}_h^* satisfy the assumption 2.3. Then the following statements hold true:*

- (i) *There exists a C^3 smooth manifold $\widetilde{\mathcal{M}}_h$, so that \mathcal{M}_h is a linear interpolation of $\widetilde{\mathcal{M}}_h$ at the vertices. Moreover, the Jacobian of the local geometric mapping at each vertex equals to the recovered geometry Jacobian using gradient recovery method.*
- (ii) *Let $\mathbf{r}_{\tau_{h,j}}$ and $\tilde{\mathbf{r}}_{\tau_{h,j}}$ be the parametrization of the curved triangular surfaces $\tau_j \subset \mathcal{M}$ and $\tilde{\tau}_{h,j} \subset \mathcal{M}_h$ from the triangle $\tau_{h,j}$, respectively. Then there is the estimate*

$$\|\partial \mathbf{r}_{\tau_{h,j}} - \partial \tilde{\mathbf{r}}_{\tau_{h,j}}\|_{\infty, \tau_{h,j}} \leq Ch^2 \quad (4.4)$$

where C is a constant independent of h .

- (iii) *Let $v : \mathcal{M} \rightarrow \mathbb{R}$ be functions in $W^{k,p}(\mathcal{M})$, and \tilde{v}_h be the pullback of v to $\widetilde{\mathcal{M}}_h$, then we have*

$$C_1 \|\tilde{v}_h\|_{W^{k,p}(\widetilde{\mathcal{M}}_h)} \leq \|v\|_{W^{k,p}(\mathcal{M})} \leq C_2 \|\tilde{v}_h\|_{W^{k,p}(\widetilde{\mathcal{M}}_h)}, \quad (4.5)$$

for some constants $0 < C_1 \leq C_2$.

Proof. (i) For the first statement, we design the following algorithm to construct the smooth manifold $\widetilde{\mathcal{M}}_h$. To simplify the illustration, we focus again on 2-dimensional manifolds.

- At each vertex x_i of \mathcal{M}_h , we use PPR algorithm [23] to recover the local geometry as a graph of a scalar function s_i for $i \in I_h$.
- For each triangle $\tau_{h,j}$ with $j \in J_h$, we build a local coordinate system, take the barycenter of $\tau_{h,j}$ as the origin, and transfer the recovered functions $\{s_i\}$ associated to $\tau_{h,j}$ to the new local coordinate, individually. Also, the gradient of s_i at the vertex x_i is calculated using the new coordinates on $\tau_{h,j}$.
- We use a 3^{rd} order polynomial to fit the function and gradient values over $\tau_{h,j}$. The data are function values at the 3 vertices (in fact with function value 0), and the gradient values of s_i at each vertex x_i which contribute 6 directional derivative values on the 3 edges of $\tau_{h,j}$. This gives 9 linearly independent equations.
- We put another constraint that the local polynomial value at the barycenter of every triangle $\tau_{h,j}$ matches the function value whose graph is the patch τ_j at the normal cross with the barycenter of $\tau_{h,j}^*$.

- We have now 10 linear independent equations in total on each triangle $\tau_{h,j}$, thus a 3^{rd} order local polynomial is uniquely determined.
- On every edge of the triangles, it is a one dimensional 3^{rd} order polynomial function which is uniquely determined by the vertices and the directional derivatives conditions. Note that polynomials at neighbored triangle edges are invariant under affine coordinate transformation. Therefore the local polynomials matches each other at every edge of neighbored triangles.
- Going through all the indexes $j \in J_h$ with the described algorithm. This gives us a closed, element-wise 3^{rd} order polynomial patches which we denote it by $\widetilde{\mathcal{M}}_h$.

To have the global smoothness, consider mollifier Φ_ϵ operator, and $\widetilde{\mathcal{M}}_h := \lim_{\epsilon \downarrow 0} \Phi_\epsilon \widetilde{\mathcal{M}}_h$. This in fact guarantees that $\widetilde{\mathcal{M}}_h$ is C^∞ smooth.

(ii) For the second statement, we notice the following relation:

$$\begin{aligned} \|\partial \mathbf{r}_{\tau_{h,j}} - \partial \tilde{\mathbf{r}}_{\tau_{h,j}}\|_{\infty, \tau_{h,j}} &\leq \|\partial \mathbf{r}_{\tau_{h,j}} - \bar{G}_h \Gamma_j^*\|_{\infty, \tau_{h,j}} + \|\bar{G}_h \Gamma_j^* - \bar{G}_h \Gamma_j\|_{\infty, \tau_{h,j}} \\ &\quad + \|\bar{G}_h \Gamma_j - \partial \tilde{\mathbf{r}}_{\tau_{h,j}}\|_{\infty, \tau_{h,j}}. \end{aligned} \quad (4.6)$$

Here we take $\tau_{h,j}$ the parameter domain for both $\mathbf{r}_{\tau_{h,j}}$ and $\tilde{\mathbf{r}}_{\tau_{h,j}}$. Γ_j^* and Γ_j are the local geometric mapping from the linear interpolations of $\mathbf{r}_{\tau_{h,j}}$ and $\tilde{\mathbf{r}}_{\tau_{h,j}}$ at the vertices of $\tau_{h,j}$, respectively. \bar{G}_h is the local PPR gradient recovery operator.

The first and the third terms on the right-hand side of (4.6) can be estimated using polynomial preserving properties of \bar{G}_h and the smoothness of the functions $\mathbf{r}_{\tau_{h,j}}$ and $\tilde{\mathbf{r}}_{\tau_{h,j}}$, which gives

$$\|\partial \mathbf{r}_{\tau_{h,j}} - \bar{G}_h \Gamma_j^*\|_{\infty, \tau_{h,j}} \leq c_1 \|\mathbf{r}_{\tau_{h,j}}\|_{3, \tau_{h,j}} h^2, \quad \|\bar{G}_h \Gamma_j - \partial \tilde{\mathbf{r}}_{\tau_{h,j}}\|_{\infty, \tau_{h,j}} \leq c_2 \|\tilde{\mathbf{r}}_{\tau_{h,j}}\|_{3, \tau_{h,j}} h^2. \quad (4.7)$$

Here \bar{G}_h is realized using the linear interpolation of the recovered gradients of s_i at the every vertices of $\tau_{h,j}$ transformed under the local coordinates on $\tau_{h,j}$. The second term on the right-hand side of (4.6) can be estimated from Lemma 4.2 and the boundedness of \bar{G}_h [17]:

$$\|\bar{G}_h \Gamma_j^* - \bar{G}_h \Gamma_j\|_{\infty, \tau_{h,j}} \leq C \|\partial \Gamma_j^* - \text{Id}\|_{\infty, \tau_{h,j}} \leq c_3 h^2. \quad (4.8)$$

Since $\|\mathbf{r}_{\tau_{h,j}}\|_{3, \tau_{h,j}}$ and $\|\tilde{\mathbf{r}}_{\tau_{h,j}}\|_{3, \tau_{h,j}}$ both are uniformly bounded, combining (4.7) and (4.8) and returning to (4.6) give the estimate

$$\|\partial \mathbf{r}_{\tau_{h,j}} - \partial \tilde{\mathbf{r}}_{\tau_{h,j}}\|_{\infty, \tau_{h,j}} \leq Ch^2.$$

(iii) For the equivalence (4.5) we can use the results in [7, page 811], which is able to show the equivalence on each triangle pairs of \mathcal{M}_h and $\widetilde{\mathcal{M}}_h$, that is

$$c_{j,1} \|\tilde{v}_h\|_{W^{k,p}(\tilde{\tau}_{h,j})} \leq \|v_h\|_{W^{k,p}(\tau_{h,j})} \leq c_{j,2} \|\tilde{v}_h\|_{W^{k,p}(\tilde{\tau}_{h,j})},$$

for some constants $\{c_{j,1}\}_{j \in J_h} > 0$ and $\{c_{j,2}\}_{j \in J_h} > 0$. The equivalence for functions defined on triangle pairs of τ_j and $\tau_{h,j}$ is similarly shown. Then we arrive the following

$$\tilde{c}_{j,1} \|\tilde{v}_h\|_{W^{k,p}(\tilde{\tau}_{h,j})} \leq \|v\|_{W^{k,p}(\tau_j)} \leq \tilde{c}_{j,2} \|\tilde{v}_h\|_{W^{k,p}(\tilde{\tau}_{h,j})}.$$

with constants $\{\tilde{c}_{j,1}\}_{j \in J_h} > 0$ and $\{\tilde{c}_{j,2}\}_{j \in J_h} > 0$. Since $\mathcal{M}_h \rightarrow \mathcal{M}$ as $h \rightarrow 0$, we have $\widetilde{\mathcal{M}}_h \rightarrow \mathcal{M}$ as well. This tells that $\tilde{c}_{j,1}, \tilde{c}_{j,2} \rightarrow 1$ as $h \rightarrow 0$, which indicates that the constants $\{\tilde{c}_{j,1}\}_{j \in J_h}$ and $\{\tilde{c}_{j,2}\}_{j \in J_h}$ are uniformly bounded. Then we derive the equivalence in (4.5). \square

In order to prove the superconvergence in the case when the vertices of \mathcal{M}_h are not located exactly on \mathcal{M} , but in a h^2 -neighborhood around it, we use the following estimate.

Lemma 4.2. *Let Assumption 2.3 hold, and let $\widetilde{\mathcal{M}}_h$ be constructed from Proposition 4.1. Let $v \in W^{3,\infty}(\mathcal{M})$, and let $\tilde{v}_h := \tilde{T}_h v$ be pullback of v from \mathcal{M} to $\widetilde{\mathcal{M}}_h$: $\tilde{v}_h(\tilde{\mathbf{r}}_{h,i}(\zeta)) = v(\mathbf{r}_i(\zeta))$ for every $\zeta \in \Omega_i$ and all $i \in I_h$, where $\tilde{\mathbf{r}}_{h,i} : \Omega_i \rightarrow \widetilde{\mathcal{M}}_{h,i}$ and $\mathbf{r}_i : \Omega_i \rightarrow \mathcal{M}_i$. Then the following estimate holds:*

$$\|\nabla_g v - (\tilde{T}_h)^{-1} \nabla_{\tilde{g}_h} \tilde{v}_h\|_{0, \mathcal{M}} \lesssim h^2 \|\nabla_g v\|_{0, \mathcal{M}}. \quad (4.9)$$

Proof. Recall (3.1) for the definition of gradient in the local parametric domain, particularly, we take the local parametric domain to be $\tau_{h,j}$. Then we have for every $j \in J_h$

$$\begin{aligned}
& \left\| \nabla_g v - (\tilde{T}_h)^{-1} \nabla_{\tilde{g}_h} \tilde{v}_h \right\|_{0,\tau_j}^2 = \int_{\tau_{h,j}} |\nabla \tilde{v} ((\partial \mathbf{r}_{\tau_{h,j}})^\dagger - (\partial \tilde{\mathbf{r}}_{\tau_{h,j}})^\dagger)|^2 \sqrt{\det(\partial \mathbf{r}_{\tau_{h,j}} (\partial \mathbf{r}_{\tau_{h,j}})^\top)} \\
& \leq \left\| \text{Id} - \partial \mathbf{r}_{\tau_{h,j}} (\partial \tilde{\mathbf{r}}_{\tau_{h,j}})^\dagger \right\|_{\infty,\tau_{h,j}}^2 \int_{\tau_{h,j}} |\nabla \tilde{v} (\partial \mathbf{r}_{\tau_{h,j}})^\dagger|^2 \sqrt{\det(\partial \mathbf{r}_{\tau_{h,j}} (\partial \mathbf{r}_{\tau_{h,j}})^\top)} \\
& = \left\| \text{Id} - \partial \mathbf{r}_{\tau_{h,j}} (\partial \tilde{\mathbf{r}}_{\tau_{h,j}})^\dagger \right\|_{\infty,\tau_{h,j}}^2 \left\| \nabla_g v \right\|_{0,\tau_j}^2.
\end{aligned} \tag{4.10}$$

Using the estimate (4.4) from Proposition 4.1, we derive that

$$\left\| \text{Id} - \partial \mathbf{r}_{\tau_{h,j}} (\partial \tilde{\mathbf{r}}_{\tau_{h,j}})^\dagger \right\|_{\infty,\tau_{h,j}} \sim \left\| \partial \mathbf{r}_{\tau_{h,j}} - \partial \tilde{\mathbf{r}}_{\tau_{h,j}} \right\|_{\infty,\tau_{h,j}} \leq Ch^2.$$

With the above estimate back to (4.10), we achieve the conclusion by summing over all the index $j \in J_h$ and then taking the square root. \square

Now we are ready to show the superconvergence of the gradient recovery on \mathcal{M}_h , which is considered to be an answer to the open question in [21].

Theorem 4.3. *Let Assumption 2.3 hold, and $u \in W^{3,\infty}(\mathcal{M})$ be the solution of (4.2), and u_h be the solution of (4.3). Then*

$$\begin{aligned}
\left\| \nabla_g u - T_h^{-1} G_h u_h \right\|_{0,\mathcal{M}} & \leq Ch^2 \left(\sqrt{\mathcal{A}(\mathcal{M})} D(g, g^{-1}) \|u\|_{3,\infty,\mathcal{M}} + \|f\|_{0,\mathcal{M}} \right) \\
& \quad + Ch^{1+\min\{1,\sigma\}} \left(\|u\|_{3,\mathcal{M}} + \|u\|_{2,\infty,\mathcal{M}} \right).
\end{aligned} \tag{4.11}$$

Proof. This is readily shown using the triangle inequality

$$\left\| \nabla_g u - T_h^{-1} G_h u_h \right\|_{0,\mathcal{M}} \leq \left\| \nabla_g u - (\tilde{T}_h)^{-1} \nabla_{\tilde{g}_h} \tilde{u}_h \right\|_{0,\mathcal{M}} + \left\| (\tilde{T}_h)^{-1} \nabla_{\tilde{g}_h} \tilde{u}_h - T_h^{-1} G_h u_h \right\|_{0,\mathcal{M}}. \tag{4.12}$$

The first part on the right hand side of (4.12) is estimated using Lemma 4.2:

$$\left\| \nabla_g u - (\tilde{T}_h)^{-1} \nabla_{\tilde{g}_h} \tilde{u}_h \right\|_{0,\mathcal{M}} \lesssim h^2 \left\| \nabla_g u \right\|_{0,\mathcal{M}}. \tag{4.13}$$

Assumption 2.3, Proposition 2.5 and Proposition 4.1 ensure that the geometric assumptions of [10, Theorem 5.3] is satisfied, i.e., the $\mathcal{O}(h^{2\sigma})$ irregular condition, and the vertices of \mathcal{M}_h is located on $\tilde{\mathcal{M}}_h$ which is C^3 smooth. Then the second term on the right hand side of (4.12) is estimated using [10, Theorem 5.3]. That gives

$$\begin{aligned}
\left\| \nabla_{\tilde{g}_h} \tilde{u}_h - \tilde{T}_h T_h^{-1} G_h u_h \right\|_{0,\tilde{\mathcal{M}}_h} & \leq \tilde{C} h^2 \left(\sqrt{\mathcal{A}(\tilde{\mathcal{M}}_h)} \tilde{D}(\tilde{g}, \tilde{g}^{-1}) \|\tilde{u}_h\|_{3,\infty,\tilde{\mathcal{M}}_h} + \|\tilde{f}\|_{0,\tilde{\mathcal{M}}_h} \right) \\
& \quad + \tilde{C} h^{1+\min\{1,\sigma\}} \left(\|\tilde{u}_h\|_{3,\tilde{\mathcal{M}}_h} + \|\tilde{u}_h\|_{2,\infty,\tilde{\mathcal{M}}_h} \right).
\end{aligned}$$

The equivalence relation from (4.5) in Proposition 4.1 gives the estimate on \mathcal{M} , which is

$$\begin{aligned}
\left\| (\tilde{T}_h)^{-1} \nabla_g u_h - T_h^{-1} G_h u_h \right\|_{0,\mathcal{M}} & \leq Ch^2 \left(\sqrt{\mathcal{A}(\mathcal{M})} D(g, g^{-1}) \|u\|_{3,\infty,\mathcal{M}} + \|f\|_{0,\mathcal{M}} \right) \\
& \quad + Ch^{1+\min\{1,\sigma\}} \left(\|u\|_{3,\mathcal{M}} + \|u\|_{2,\infty,\mathcal{M}} \right).
\end{aligned} \tag{4.14}$$

Using embedding theorem that the right-hand side of (4.13) can actually be bounded by the first term on the right-hand side of (4.14). The proof is concluded by putting (4.13) and (4.14) together. \square

5 Numerical results

In this section, we present two numerical examples to verify the theoretical analysis. The first example is on unit sphere, where we add artificial $\mathcal{O}(h^2)$ perturbation to the discretized mesh in

order to verify our theoretical results. With this, we are able to verify the geometric approximation of \mathcal{M}_h to \mathcal{M}_h^* . The second example is on a general surface, where the vertices of its discretization mesh do not located on the exact surface. The initial mesh of the general surface was generated using the three-dimensional surface mesh generation module of the Computational Geometry Algorithms Library [20]. To get meshes in other levels, we first perform the uniform refinement. Then we project the newest vertices onto the \mathcal{M} . In the general case, there is no explicit project map available. Hence we adopt the first-order approximation of projection map as given in [8]. Thus, the vertices of the meshes are not on the exact surface \mathcal{M} but in an h^2 neighborhood for the second example.

We consider two different members in the family of Algorithm 1: (i) Parametric polynomial preserving recovery denoted by G_h^{pppr} , a generalization of PPR method, and (ii) Parametric superconvergent patch recovery denoted by G_h^{pspr} , a generalization of ZZ-scheme. For the sake for simplifying the notation, we define:

$$\begin{aligned} De^* &= \|T_h \nabla_g u - \nabla_{g_h} u_h\|_{0, \mathcal{M}_h^*}, & De &= \|T_h \nabla_g u - \nabla_{g_h} u_h\|_{0, \mathcal{M}_h}, \\ De_I^* &= \|\nabla_{g_h} u_I - \nabla_{g_h} u_h\|_{0, \mathcal{M}_h^*}, & De_I &= \|\nabla_{g_h} u_I - \nabla_{g_h} u_h\|_{0, \mathcal{M}_h}, \\ De_r^* &= \|T_h \nabla_g u - G_h^{pppr} u_h\|_{0, \mathcal{M}_h^*}, & De_r &= \|T_h \nabla_g u - G_h^{pppr} u_h\|_{0, \mathcal{M}_h}, \\ De_{r_2}^* &= \|T_h \nabla_g u - G_h^{pspr} u_h\|_{0, \mathcal{M}_h^*}, & De_{r_2} &= \|T_h \nabla_g u - G_h^{pspr} u_h\|_{0, \mathcal{M}_h}; \end{aligned}$$

where u_h is the finite element solution, u is the analytical solution and u_I is the linear finite element interpolation of u . We also remind that \mathcal{M}_h^* denotes the exact interpolation of \mathcal{M} .

5.1 Numerical example on unit sphere

We test with numerical solutions of Laplace-Beltrami equation on the unit sphere. The right hand side function f is chosen to fit the exact solution $u = x_1 x_2$. For the unit sphere, it is rather simple to generate meshes, denoted by \mathcal{M}_h^* , whose vertices are located on the exact surface. To validate the geometric supercloseness result and illustrate the performance of the isoparametric gradient recovery methods on discretized manifolds, we artificially add $\mathcal{O}(h^2)$ perturbation along normal directions at each vertices of \mathcal{M}_h^* and denote the resulting deviated mesh by \mathcal{M}_h . In the test example, the magnitude of the perturbation is chosen as $(-1)^i 0.01 h^2$, where i is the numbering of the node.

We provide first a numerical verification of the geometric supercloseness property. We compute the maximal norm of $\partial \mathbf{r}_h - \partial \mathbf{r}_h^*$ over all elements of the above two meshes. The numerical errors are displayed in the Table 1. Clearly, the maximal norm decays at a rate of $\mathcal{O}(h^2)$. The observed second order convergence rates are matched with the theoretical result in the Proposition 2.5.

Table 1: Result of Geometric supercloseness

Dof	12	42	162	642	2562	10242	40962
$\ \partial \mathbf{r}_h - \partial \mathbf{r}_h^*\ _\infty$	1.18e-02	7.07e-03	2.07e-03	5.40e-04	1.36e-04	3.42e-05	8.55e-06
Order	–	0.82	1.82	1.95	1.99	2.00	2.00

Then, we solve the Laplace-Beltrami equation on both \mathcal{M}_h^* and \mathcal{M}_h and the numerical performances are tabulated in Table 2. For finite element gradient error, the expected optimal convergence rate $\mathcal{O}(h)$ can be observed on both the meshes \mathcal{M}_h^* and \mathcal{M}_h . We concentrate to the finite element supercloseness error. On both \mathcal{M}_h^* and \mathcal{M}_h , we observe $\mathcal{O}(h^{1.9})$ supercloseness results. It gives solid evidence that the $\mathcal{O}(h^{2\sigma})$ irregular condition also holds true for the perturbed mesh \mathcal{M}_h . For the recovered gradient error, we observed almost the same $\mathcal{O}(h^2)$ superconvergence rates on both discretized surfaces using isoparametric gradient recovery schemes. Especially the result using parametric polynomial preserving recovery reaches the superconvergence rates $\mathcal{O}(h^{1.99})$ and $\mathcal{O}(h^{1.95})$ on \mathcal{M}_h^* and \mathcal{M}_h , respectively, which validates Theorem 4.3. The numerical results of using isoparametric superconvergent patch recovery shows superconvergence rate $\mathcal{O}(h^{1.96})$ and $\mathcal{O}(h^{1.93})$ on \mathcal{M}_h^* and \mathcal{M}_h , respectively, which indicates that it is also a valid algorithm.

Table 2: Numerical results of solving Laplace-Beltrami equation on the sphere

Dof	De^*	Order	De_I^*	Order	De_r^*	Order	$De_{r_2}^*$	Order
12	1.04e+00	-	7.93e-01	-	1.26e+00	-	1.26e+00	-
42	7.46e-01	0.53	1.14e-01	3.09	6.92e-01	0.96	6.92e-01	0.96
162	3.90e-01	0.96	3.66e-02	1.69	2.07e-01	1.79	2.07e-01	1.79
642	1.97e-01	0.99	1.05e-02	1.82	5.44e-02	1.94	5.45e-02	1.94
2562	9.90e-02	1.00	2.88e-03	1.87	1.39e-02	1.98	1.39e-02	1.97
10242	4.95e-02	1.00	7.75e-04	1.89	3.49e-03	1.99	3.55e-03	1.97
40962	2.48e-02	1.00	2.06e-04	1.91	8.78e-04	1.99	9.10e-04	1.96
Dof	De	Order	De_I	Order	De_r	Order	De_{r_2}	Order
12	1.04e+00	-	7.93e-01	-	1.26e+00	-	1.26e+00	-
42	7.46e-01	0.53	1.15e-01	3.08	6.92e-01	0.96	6.92e-01	0.96
162	3.90e-01	0.96	3.68e-02	1.69	2.07e-01	1.79	2.07e-01	1.79
642	1.97e-01	0.99	1.05e-02	1.83	5.45e-02	1.94	5.45e-02	1.94
2562	9.90e-02	1.00	2.88e-03	1.87	1.39e-02	1.97	1.40e-02	1.97
10242	4.96e-02	1.00	7.75e-04	1.89	3.53e-03	1.98	3.58e-03	1.97
40962	2.48e-02	1.00	2.06e-04	1.91	9.16e-04	1.95	9.42e-04	1.93

5.2 Numerical example on general surface

In this example, we consider a general surface which can be represented as the zero level-set of the following function

$$\Phi(x) = (x^2 - 1)^2 + (y^2 - 1)^2 + (z^2 - 1)^2 - 1.05.$$

We solve the Laplace-Beltrami equation

$$-\Delta_g u + u = f;$$

with the exact solution $u = \exp(x^2 + y^2 + z^2)$. The right hand side function f is computed from u .

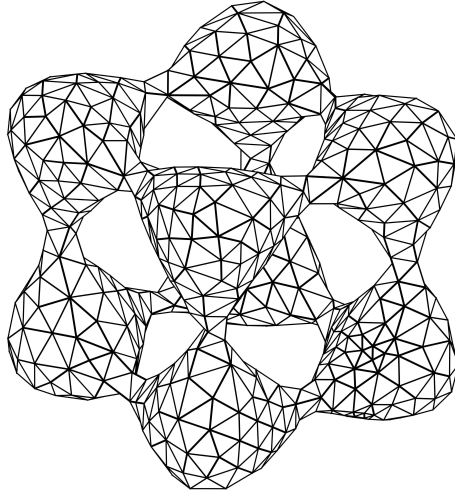


Figure 2: Initial mesh on a general surface

In this case, the vertices of the triangles \mathcal{M}_h using the mentioned mesh generating algorithm are located in the $\mathcal{O}(h^2)$ neighborhood of the exact surface. The first level of mesh is plotted in Figure 2. The history of numerical errors is documented in Table 3. As expected, we can observe the $\mathcal{O}(h)$ optimal convergence rate for the finite element gradient. The rate $\mathcal{O}(h^{1.9})$ can be observed for the error between the finite element gradient and the gradient of the interpolation of the exact solution. Again, it means the mesh \mathcal{M}_h satisfies the $\mathcal{O}(h^{2\sigma})$ irregular condition. As depicted by the Theorem 4.3, the recovered gradient using parametric polynomial preserving recovery is

superconvergent to the exact gradient at the rate of $\mathcal{O}(h^2)$ even though the vertices are not located on the exact surface. For parametric superconvergent patch recovery, it deteriorates a little bit but we can still observe $\mathcal{O}(h)^{1.86}$ superconvergence.

Table 3: Numerical results of solving Laplace-Beltrami equation on a general surface

Dof	De	Order	De_I	Order	De_r	Order	De_{r_2}	Order
701	1.32e+01	–	5.67e+00	–	1.12e+01	–	1.19e+01	–
2828	6.93e+00	0.93	1.67e+00	1.75	3.66e+00	1.61	3.68e+00	1.69
11336	3.52e+00	0.98	4.89e-01	1.77	1.04e+00	1.81	1.06e+00	1.80
45368	1.77e+00	0.99	1.34e-01	1.87	2.76e-01	1.91	2.88e-01	1.87
181496	8.86e-01	1.00	3.54e-02	1.92	7.12e-02	1.96	7.77e-02	1.89
726008	4.43e-01	1.00	9.21e-03	1.94	1.81e-02	1.98	2.15e-02	1.86

6 Conclusion

In this paper, we concentrate on analyzing the superconvergence of gradient recovery methods on discretized manifolds whose vertices are not necessarily located on the underline exact surface. By introducing and establishing the concept of geometric supercloseness, we are entitled the capability to prove superconvergence of isoparametric polynomial preserving recovery without any prior knowledge of the exact surfaces. Numerical examples are presented to validate the theoretical findings.

Acknowledgement

GD has been partially supported by the German Research Foundation under Germany’s Excellence Strategy: The Berlin Mathematics Research Center MATH+ (EXC-2046/1, project ID: 390685689). HG was partially supported by Andrew Sisson Fund of the University of Melbourne.

References

- [1] M. AINSWORTH AND J. T. ODEN, *A posteriori error estimation in finite element analysis*, Pure and Applied Mathematics (New York), Wiley-Interscience [John Wiley & Sons], New York, 2000.
- [2] T. AUBIN, *Best constants in the Sobolev imbedding theorem: the Yamabe problem*, in Seminar on Differential Geometry, vol. 102 of Ann. of Math. Stud., Princeton Univ. Press, Princeton, N.J., 1982, pp. 173–184.
- [3] R. E. BANK AND J. XU, *Asymptotically exact a posteriori error estimators. I. Grids with superconvergence*, SIAM J. Numer. Anal., 41 (2003), pp. 2294–2312 (electronic).
- [4] S. C. BRENNER AND L. R. SCOTT, *The mathematical theory of finite element methods*, vol. 15 of Texts in Applied Mathematics, Springer, New York, third ed., 2008.
- [5] H. CHEN, H. GUO, Z. ZHANG, AND Q. ZOU, *A C^0 linear finite element method for two fourth-order eigenvalue problems*, IMA J. Numer. Anal., 37 (2017), pp. 2120–2138.
- [6] P. G. CIARLET, *The finite element method for elliptic problems*, vol. 40 of Classics in Applied Mathematics, Society for Industrial and Applied Mathematics (SIAM), Philadelphia, PA, 2002. Reprint of the 1978 original [North-Holland, Amsterdam; MR0520174 (58 #25001)].
- [7] A. DEMLOW, *Higher-order finite element methods and pointwise error estimates for elliptic problems on surfaces*, SIAM J. Numer. Anal., 47 (2009), pp. 805–827.

- [8] A. DEMLOW AND G. DZIUK, *An adaptive finite element method for the Laplace-Beltrami operator on implicitly defined surfaces*, SIAM J. Numer. Anal., 45 (2007), pp. 421–442 (electronic).
- [9] M. P. DO CARMO, *Riemannian geometry*, Mathematics: Theory & Applications, Birkhäuser Boston, Inc., Boston, MA, 1992. Translated from the second Portuguese edition by Francis Flaherty.
- [10] G. DONG AND H. GUO, *Parametric polynomial preserving recovery on manifolds*, arXiv preprint, (2019), pp. 1 – 27.
- [11] G. DONG, B. JÜTTLER, O. SCHERZER, AND T. TAKACS, *Convergence of Tikhonov regularization for solving ill-posed operator equations with solutions defined on surfaces*, Inverse Probl. Imaging, 11 (2017), pp. 221 – 246.
- [12] Q. DU AND L. JU, *Finite volume methods on spheres and spherical centroidal Voronoi meshes*, SIAM J. Numer. Anal., 43 (2005), pp. 1673–1692 (electronic).
- [13] J. GRANDE AND A. REUSKEN, *A higher order finite element method for partial differential equations on surfaces*, SIAM J. Numer. Anal., 54 (2016), pp. 388–414.
- [14] H. GUO AND Z. ZHANG, *Gradient recovery for the Crouzeix-Raviart element*, J. Sci. Comput., 64 (2015), pp. 456–476.
- [15] H. GUO, Z. ZHANG, AND Q. ZOU, *A C^0 Linear Finite Element Method for Biharmonic Problems*, J. Sci. Comput., 74 (2018), pp. 1397–1422.
- [16] A. M. LAKHANY, I. MAREK, AND J. R. WHITEMAN, *Superconvergence results on mildly structured triangulations*, Comput. Methods Appl. Mech. Engrg., 189 (2000), pp. 1–75.
- [17] A. NAGA AND Z. ZHANG, *A posteriori error estimates based on the polynomial preserving recovery*, SIAM J. Numer. Anal., 42 (2004), pp. 1780–1800 (electronic).
- [18] ———, *Function value recovery and its application in eigenvalue problems*, SIAM J. Numer. Anal., 50 (2012), pp. 272–286.
- [19] A. NAGA, Z. ZHANG, AND A. ZHOU, *Enhancing eigenvalue approximation by gradient recovery*, SIAM J. Sci. Comput., 28 (2006), pp. 1289–1300.
- [20] L. RINEAU AND M. YVINEC, *3D surface mesh generation*, in CGAL User and Reference Manual, CGAL Editorial Board, 4.9 ed., 2016.
- [21] H. WEI, L. CHEN, AND Y. HUANG, *Superconvergence and gradient recovery of linear finite elements for the Laplace-Beltrami operator on general surfaces*, SIAM J. Numer. Anal., 48 (2010), pp. 1920–1943.
- [22] J. XU AND Z. ZHANG, *Analysis of recovery type a posteriori error estimators for mildly structured grids*, Math. Comp., 73 (2004), pp. 1139–1152 (electronic).
- [23] Z. ZHANG AND A. NAGA, *A new finite element gradient recovery method: superconvergence property*, SIAM J. Sci. Comput., 26 (2005), pp. 1192–1213 (electronic).
- [24] O. C. ZIENKIEWICZ AND J. Z. ZHU, *The superconvergent patch recovery and a posteriori error estimates. I. The recovery technique*, Internat. J. Numer. Methods Engrg., 33 (1992), pp. 1331–1364.
- [25] ———, *The superconvergent patch recovery and a posteriori error estimates. II. Error estimates and adaptivity*, Internat. J. Numer. Methods Engrg., 33 (1992), pp. 1365–1382.